UNIVERSITY OF BIRMINGHAM
University of Birmingham Research at Birmingham

The response of embedded strain sensors in concrete beams subjected to thermal loading

Ge, Yu; Elshafie, Mohammed Z. E. B.; Dirar, Samir; Middleton, Campbell R.

DOI:
10.1016/j.conbuildmat.2014.07.102

License:
None: All rights reserved

Document Version
Early version, also known as pre-print

Citation for published version (Harvard):
Ge, Y, Elshafie, MZEB, Dirar, S & Middleton, CR 2014, 'The response of embedded strain sensors in concrete beams subjected to thermal loading', *Construction and Building Materials*, vol. 70, pp. 279-290. https://doi.org/10.1016/j.conbuildmat.2014.07.102

Link to publication on Research at Birmingham portal

Publisher Rights Statement:
NOTICE: this is the author's version of a work which was accepted for publication in Construction and Building Materials. Changes resulting from the publishing process, such as peer review, editing, corrections, structural formatting, and other quality control mechanisms may not be reflected in this document. Changes may have been made to this work since it was submitted for publication. A definitive version was subsequently published in Construction and Building Materials , Vol 70, November 2014, pp. 279-90.
DOI: 10.1016/j.conbuildmat.2014.07.102

Eligibility for repository checked January 2015

General rights
Unless a licence is specified above, all rights (including copyright and moral rights) in this document are retained by the authors and/or the copyright holders. The express permission of the copyright holder must be obtained for any use of this material other than for purposes permitted by law.

•Users may freely distribute the URL that is used to identify this publication.
•Users may download and/or print one copy of the publication from the University of Birmingham research portal for the purpose of private study or non-commercial research.
•User may use extracts from the document in line with the concept of 'fair dealing' under the Copyright, Designs and Patents Act 1988 (?)
•Users may not further distribute the material nor use it for the purposes of commercial gain.

Where a licence is displayed above, please note the terms and conditions of the licence govern your use of this document.

When citing, please reference the published version.

Take down policy
While the University of Birmingham exercises care and attention in making items available there are rare occasions when an item has been uploaded in error or has been deemed to be commercially or otherwise sensitive.

If you believe that this is the case for this document, please contact UBIRA@lists.bham.ac.uk providing details and we will remove access to the work immediately and investigate.

Download date: 25. Apr. 2024

*Manuscript
Click here to download Manuscript: Manuscript-reivised.docx Click here to view linked References

The Response of Embedded Strain Sensors in Concrete Beams Subjected to Thermal Loading

Yu Ge[1] (Corresponding Author), Mohammed Z. E. B. Elshafie[2], Samir Dirar[3] and Campbell R. Middleton[2]

Abstract

A wide range of commercially available sensors are frequently used to record the response of civil engineering structures that may be subjected to unexpected loading scenarios, changes of environmental conditions or material deterioration. However, a common problem faced when using these sensors is to distinguish strain changes experienced by the structure due to a temperature change from strain changes that occur due to other causes. Temperature effects on strain sensors are usually accommodated by allowing for temperature effects (temperature compensation); however, there is limited research in the literature that investigates the performance of strain sensor measurements when subjected to temperature change. Understanding the temperature effect on strain sensors will greatly enhance the ability of civil engineers to monitor the performance of structural materials. In this paper, different types of commonly used and advanced strain sensors have been installed in a reinforced concrete beam to measure the thermal strain response of concrete under different temperature conditions. The experimental results demonstrated a 25-30% difference in strain measurements from the different sensors. It is shown in this paper that this difference is due to the combined effects of sensor inaccuracy, uncertainties related to the testing conditions and uncertainties associated with the temperature compensation methods.

Key words:
Concrete behaviour, Strain sensors, temperature compensation, Fibre Bragg Gratings, Brillouin backscattering, optical fibre sensors, vibrating wire strain gauges, thermal loading

[1] Ms. Yu Ge, 226/1 Acacia Place, Abbotsford, Victoria 3067, Australia. Tel: +61449859187, Email: yu.ge0427@gmail.com

[2] University of Cambridge, The Laing O'Rourke Centre for Construction Engineering and Technology, Department of Engineering, Trumpington Street, Cambridge, CB2 1PZ, United Kingdom

[3] University of Birmingham, School of Civil Engineering, Edgbaston, Birmingham B15 2TT, United Kingdom

1. Introduction

Structural Health Monitoring (SHM) relies on the use of sensors to measure physical parameters. The strain change of structures is one of the most commonly assessed quantities in SHM to investigate the performance of structures under loading. There are three categories of commercially available strain sensors: (i) discrete strain sensors, (ii) quasi-distributed strain sensors and (iii) highly distributed strain sensors. Discrete sensors measure localised strain at the point where the sensor is installed while the highly distributed strain sensors measure the complete strain profile along the entire length of the sensor. Quasi-distributed strain sensors are discrete sensors connected in series. Measurements from these sensors are adversely affected by the surrounding environment such as temperature change which induces a thermal component in the sensor strain measurement. This is due to the different thermal expansion properties of the materials that constitute the sensor itself and the structural material in which the sensor is installed. Many civil engineering structures are subjected to repeated temperature changes on a very frequent basis hence it is important to understand how the thermal effects influence the strain measurements so that the mechanical strain induced by any unexpected loading scenarios or rapid material deterioration can be more accurately derived.

The effect of temperature on different sensors (conventional and advanced) has been researched by a number of researchers in the past. The following sections will briefly discuss some of the most significant research that has been done previously. Neild et al. (2005) conducted theoretical calculations to express the relationship between the measurements of Vibrating Wire Strain Gauges (VWSG) and the thermal deformation of a test specimen. Based on the results obtained, they argued that an unstrained VWSG (i.e. free from structural material deformations but under the same environmental conditions as the test specimen) should be used as a dummy gauge to compensate the temperature effect. However, they also found that if the sizes and geometries of the test specimens and the control samples were

significantly different, they would be affected differently by temperature. This may have a significant implication, particularly in cases where such sensors are embedded in massive concrete structures like bridges for example. Sreeshyiarn et al. (2008) reported a temperature calibration factor of 2.19με/°C for an embedded VWSG and 4.32με/°C for a surface mounted gauge on a concrete specimen. They expressed concern that, due to the varied thermal expansion coefficient of concrete from one case to another, an individual calibration test was required for each VWSG.

Recently developed measurement technologies, such as fibre optic sensors, have been used to measure strain and/or temperature changes of structures whether embedded internally or attached externally. The advantages of these sensors over conventional sensors (e.g. VWSGs) include: they are not affected by electro-magnetic fields, longer sensing lengths and the potential to provide a long term reliable monitoring solution (Chen et. al., 1994). Two types of fibre optic sensors are most commonly adopted in practice: (a) the Fibre Bragg Grating sensors (FBG) and the distributed optical fibre cables (FO). The former are quasi-distributed sensors where individual FBGs can be placed at numerous locations on one cable (providing simultaneous multiple points sensing) while the latter have the advantage of providing highly-distributed continuous strain profiles along the entire length of the optical fibre cables and are believed to have potential for long term monitoring with less implementation costs (Hoult et al. 2009). The particular FO technique discussed in this paper uses the Brillouin backscattering technique (Bao and Chen, 2011). Published case studies in the literature where temperature compensation is discussed in detail are very limited. Rodrigues et al. (2010) presented a study on FBG sensors where the FBG sensors were initially fixed onto steel tubes before they were embedded in the concrete deck of the Lezíria Bridge in Portugal. For temperature compensation in particular, the paper mentioned briefly that a direct calculation could be applied with known temperature measurements at the location of the FBG sensors, taking into account the characteristics of the FBGs and the material of the structure that was

being monitored. However, no further detail was given for the accuracy and reliability of measurements after applying such a temperature compensation method. Mohamad (2008) discussed the use of dummy temperature optical fibre cables alongside the active FO sensing cables to carry out temperature compensation for distributed FO measurements. The design of the temperature optical fibre cable allows the cables to be used for temperature compensation. The fibre core in the FO dummy temperature cable can expand freely in a gel-filled tube and hence is isolated from any strains transmitted to the outer sheath of the cable. The "temperature strain" measured by the temperature cable is then subtracted from the total strain measured by the active FO sensing cable to calculate the mechanical strain. Mohamad (2012) argued that using such a method is much cheaper and simpler than other approaches, particularly when temperature coefficients relating to different types of optical fibres can be easily estimated. Field case studies conducted recently (Webb, 2010 and Schwamb, 2010) discussed the installation of FO temperature and strain cables in a number of pre-stressed concrete bridge beams and cast in-situ concrete pile foundations at the Nine Wells Bridge near Cambridge, UK. Schwamb (2010), who reported the pile foundation sensing results, pointed out that the accurate interpretation of the measurements, including temperature compensation, is highly dependent on the geometric alignment of the strain and temperature cables; a small mis-alignment of 5cm resulted in significantly inaccurate results. Webb (2010) adopted the same temperature compensation method as suggested by Mohamad (2012) and compared the temperature compensated FO measurements to the theoretical strain prediction and found that the two were correlated well in larger scale.

In summary, SHM schemes have been used to monitor the performance of a number of civil engineering structures, however, in most cases the sensors employed in these SHM schemes are likely to be subjected to and affected by temperature changes. In most studies in the literature, measurements from different independent instruments would normally be introduced to allow cross calibration and

comparison, however there is still little quantitative evidence available on the reliability of the different sensors when subjected to temperature changes. Understanding the effect of the temperature changes on the different strain sensors plays a significant role in understanding the performance of the structures under conditions such as unexpected/extreme loading scenarios and rapid material deterioration. The research presented in this paper provides quantitative information about the effect of temperature on some of the most commonly used strain sensors such as the VWSGs and FBGs, as well as some of the promising new strain sensors such as distributed FO sensors.

2. Experiment design

Since the vast majority of commonly used strain sensors are affected to some extent by temperature, the reliability of their output measurements needs careful calibration and validation. Therefore, a thorough study of the effect of temperature on strain measurements is needed. The research presented in this paper examined the performance of strain sensors from two main perspectives:

1) How reliable is the sensor calibration and what is the accuracy of the measurements?
2) What role does temperature compensation play in the accuracy of measurements?

To investigate the questions above, an experimental programme was conducted in which a reinforced concrete beam, instrumented with four types of strain sensors, was subjected to varied temperature conditions without external mechanical loading. The beam was 3.5m in length with cross-section dimensions of 25cm in depth and 20cm in width as shown in Figure 1. It had a cylinder compressive strength of 32 MPa at 28 days. Four Grade 500B reinforcement steel bars with a diameter of 12mm were used as longitudinal reinforcement while 8mm diameter shear links were used (at a spacing of 15cm towards the supports 50cm elsewhere) along the beam. The concrete cover was 20mm from the

surface of the beam to the surface of shear links. The beam was simply supported at each end with the roller bearings allowing free expansion in the longitudinal direction. Four types of sensors were installed: a conventional foil electrical resistance strain gauge (ERS), a Vibrating Wire Strain Gauge (VWSG), Fibre Bragg Grating sensors (FBG) and distributed Brillouin backscattering optical fibre sensor (FO). The four types of strain sensors were located so that the point sensors (ERS, VWSG and FBG) could be used to compare results with those obtained with the distributed fibre optic sensor (FO). The location of the different sensors in the beam is shown in Figure 1c and 1d. Temperatures inside the beam were monitored by thermocouples (type K) and distributed optical fibre (FO) temperature cable. Thermocouples were installed at the same locations as each of the discrete strain sensors (ERS, VWSG and FBG) and also at the mid-height of the beam at a number of locations along the beam as shown in Figure 2a and 2b.

a) Elevation View

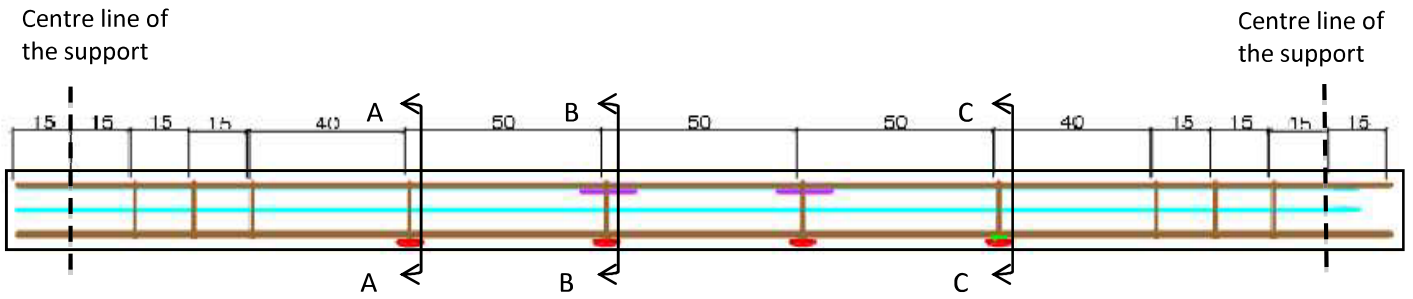

b) Top View

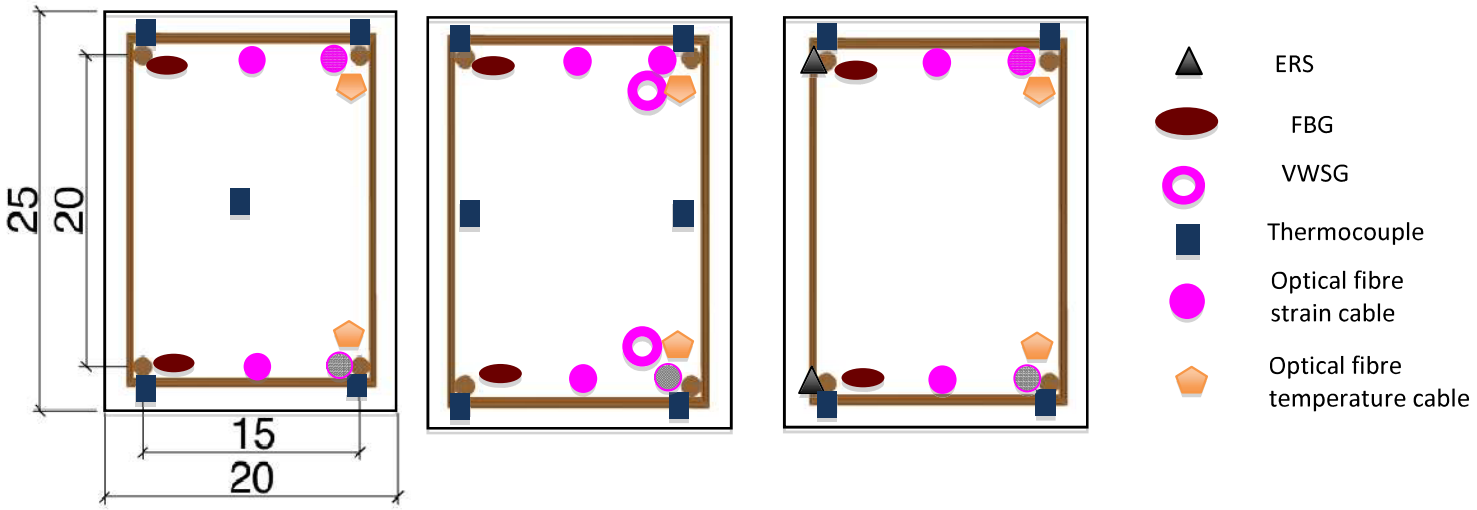

Section A-A

Section B-B

Section C-C

c) Cross sections of beam

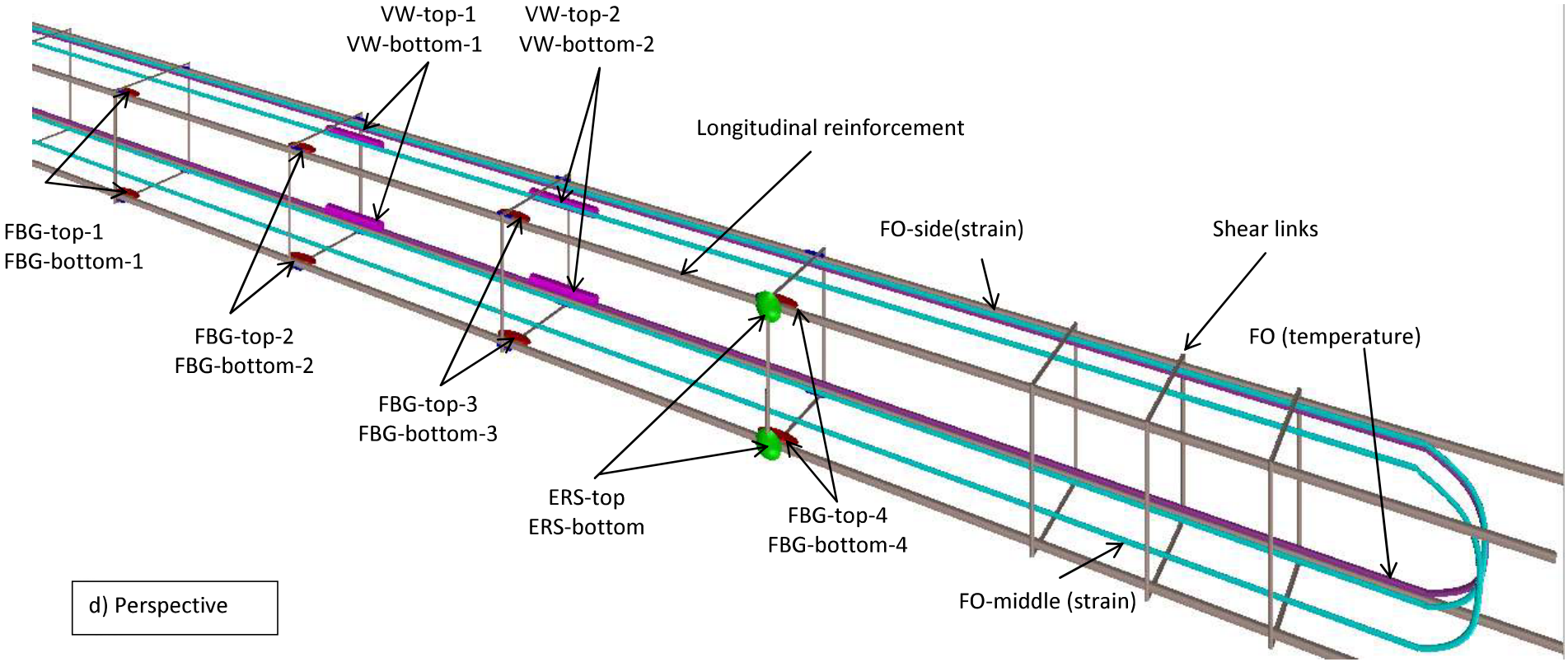

Figure 1 Schematic diagram of sensor instrumentation (All dimensions in CM)

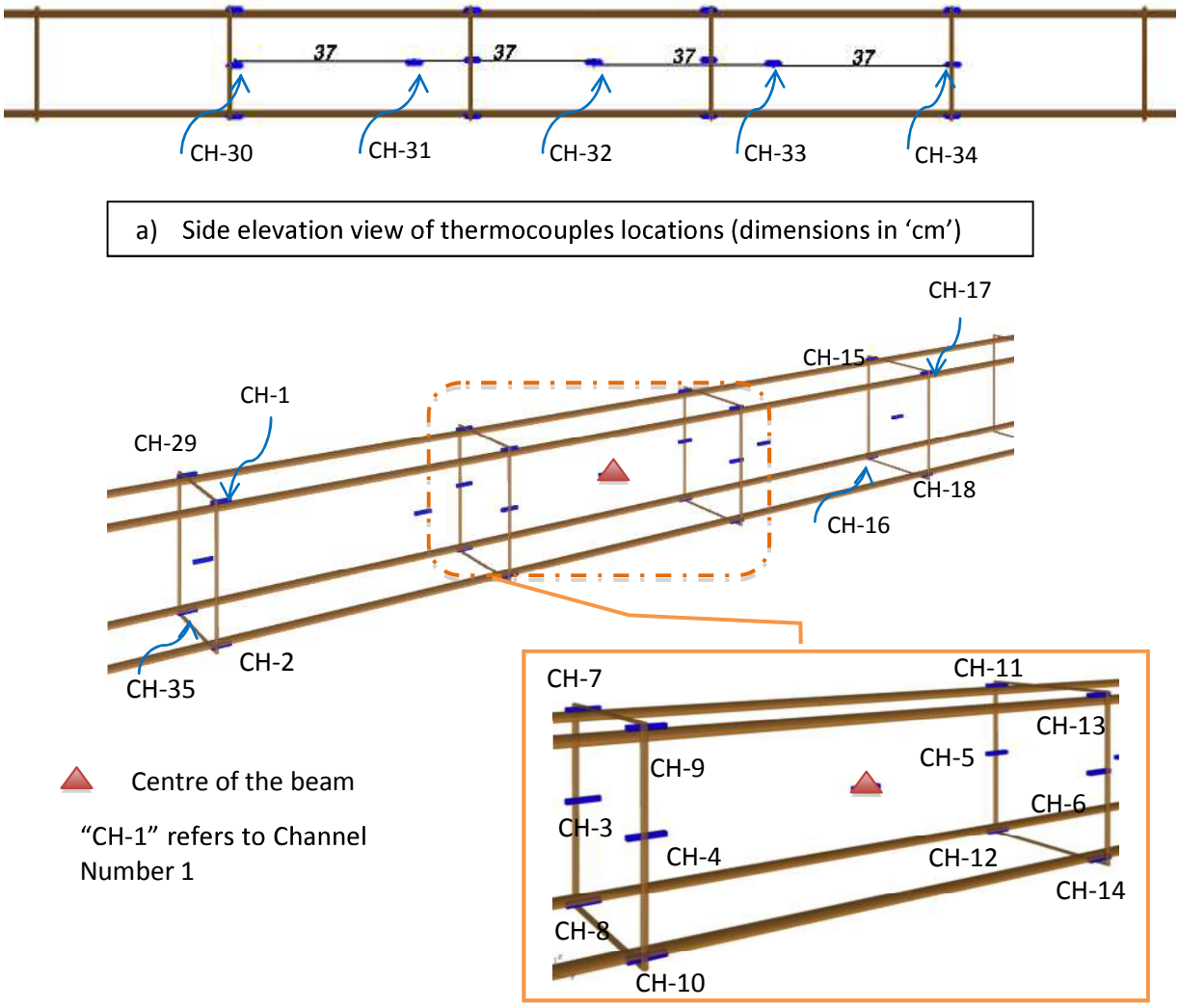

Figure 2 Location of thermocouples

The experiment was divided into two parts; firstly, the whole beam was enclosed in an insulated box where all external surfaces of the beam were uniformly heated (from room temperature up to a maximum of 40°C in 1°C increments) as shown schematically in Figure 3a. In this case, the thermal strains measured from all instruments were expected to be the same given the beam was allowed to expand freely. In the second part of the experiment, the same concrete beam was used however, this time only the top surface of the beam was exposed to rising temperature inside the temperature box (Figure 3b), thus creating a temperature gradient through the depth of the beam. The bottom was

uncovered and exposed to ambient air temperature. The ends of the beam were wrapped with glass wool insulation which allows the beam to expand freely but prevents heat lost through ends. This part of the experiment was aimed at simulating the thermal loading experienced by bridge decks (where sunlight heats up the top surface of the bridge while the bottom surface is shaded).

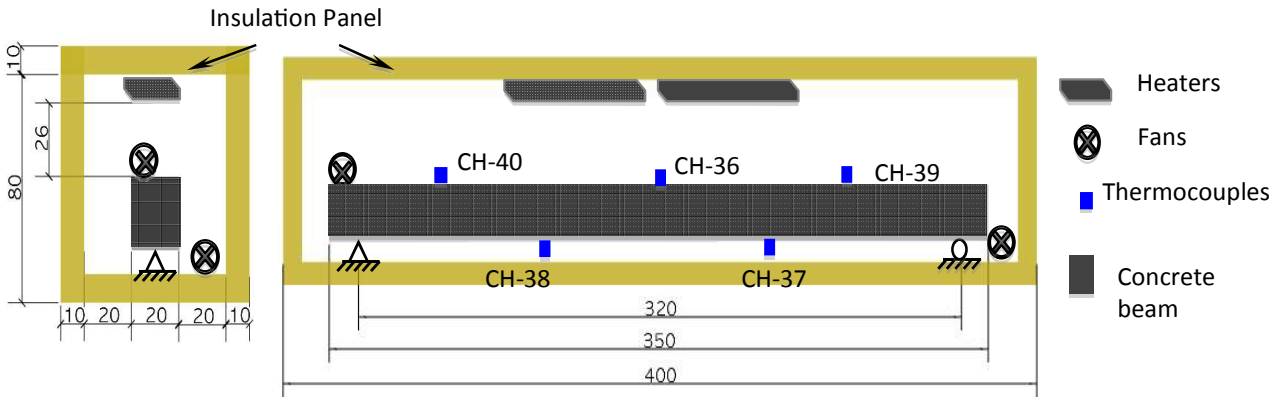

a) The constant temperature experiment

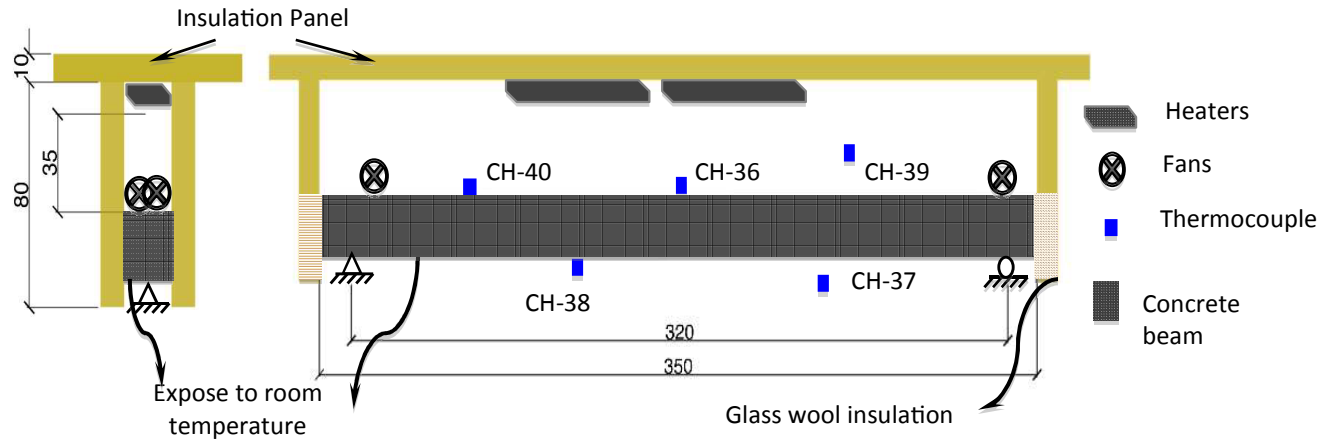

b) The temperature gradient experiment

Figure 3 Schematic experimental setups (All dimensions are in CM)

Figure 4a and 4b show images of the experimental setup for the constant temperature test. Figure 4a shows an overview of the overall experimental setup while Figure 4b shows the different parts used to control the temperature imposed on the beam surfaces. Two 120 watt heaters were used to control the

temperature inside the experimental setup, with two fans used to circulate the air within the box. In order to achieve uniform temperature conditions around the concrete beam, a number of preliminary tests were conducted to optimise the location of the heaters and the fans; **Error! Reference source not found.**b show their final locations. Figure 5a, 5b and 5c show the experimental setup for the temperature gradient test. The external fan shown in Figure 5a was used to increase the airflow at the bottom surface of the beam. This is to ensure that a distinctive temperature gradient is created. Insulation was firmly attached to the two sides of the beam to ensure only the top surface of the beam was affected by temperature change. Figure 5c shows an image of the setup inside the insulated box.

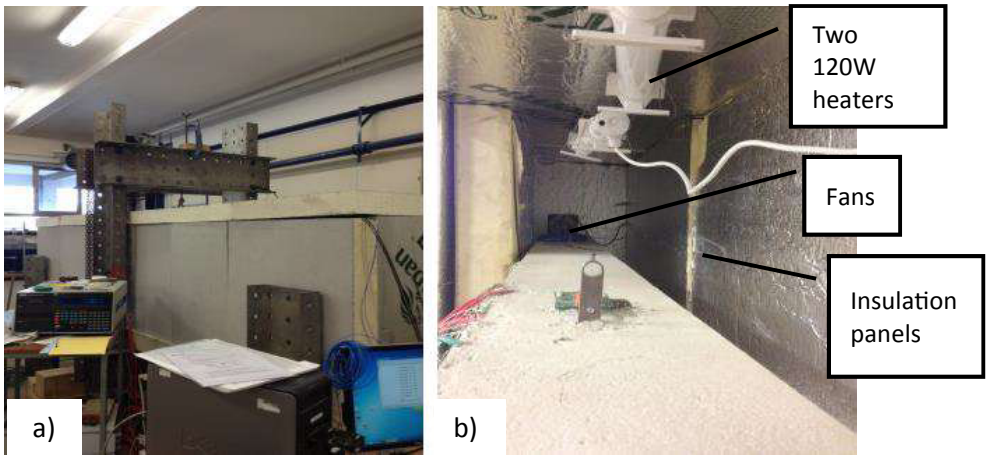

Figure 4 Experimental setup for constant temperature test

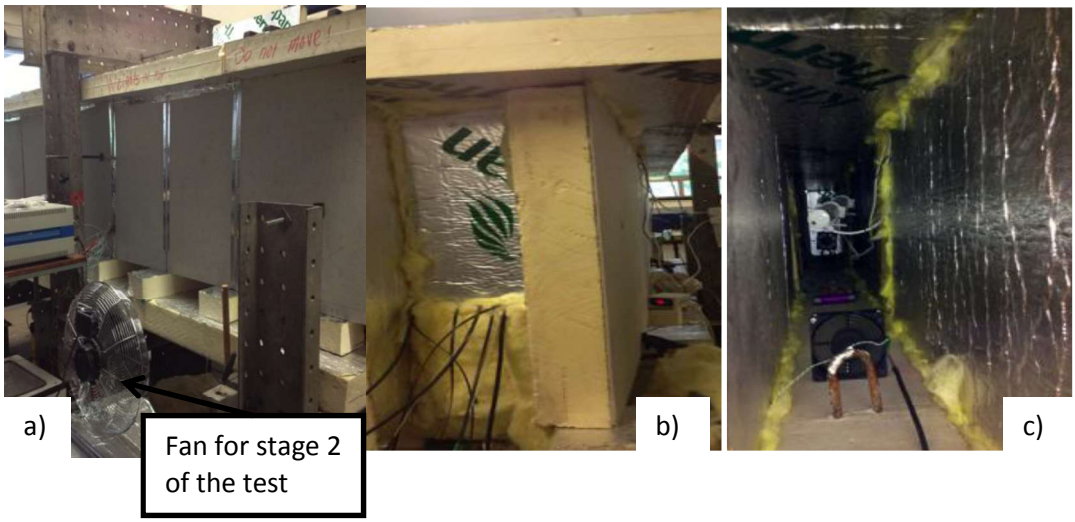

Figure 5 Experimental setup for temperature gradient test

3. Experimental Results

3.1. Constant temperature experiment

The temperature monitoring results at the locations shown in Figure 2 inside the concrete beam and at the locations shown in Figure 3a on the external surface of the beam are presented in Figure 6a and 6b. The consistency of temperature measurements along the beam span leads to the conclusion that the beam is exposed to uniformly distributed temperature all the time. Consequently, the mean temperature taken from all measurement points is representative of the temperature everywhere in the beam. The temperature difference between the core and the surroundings of the concrete beam became insignificant within 20 hours of the start of the test as shown in Figure 6c. The box temperature is the average reading of the external thermocouples shown in Figure 3a while the concrete temperature is the average reading of thermocouples show in Figure 2.

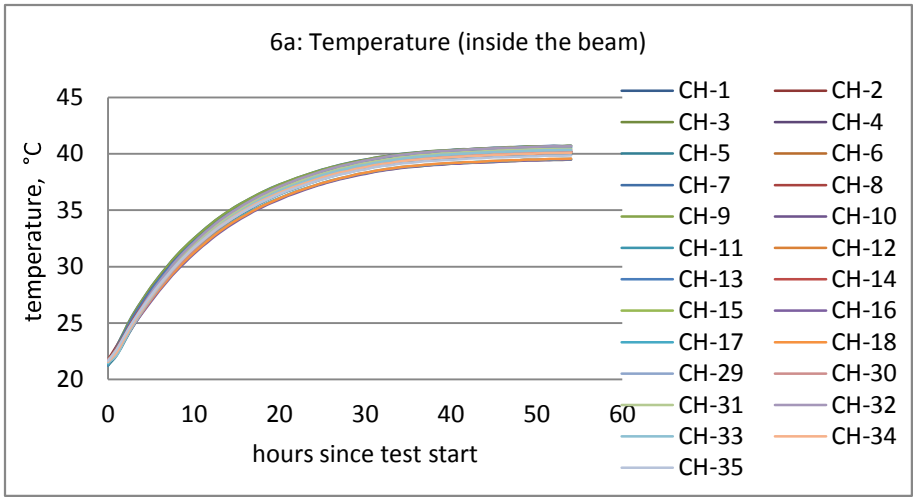
6a: Temperature (inside the beam)
temperature, °C
45
40
35
30
25
20
0
10
20
30
40
50
60
hours since test start
CH-1
CH-2
CH-3
CH-4
CH-5
CH-6
CH-7
CH-8
CH-9
CH-10
CH-11
CH-12
CH-13
CH-14
CH-15
CH-16
CH-17
CH-18
CH-29
CH-30
CH-31
CH-32
CH-33
CH-34
CH-35

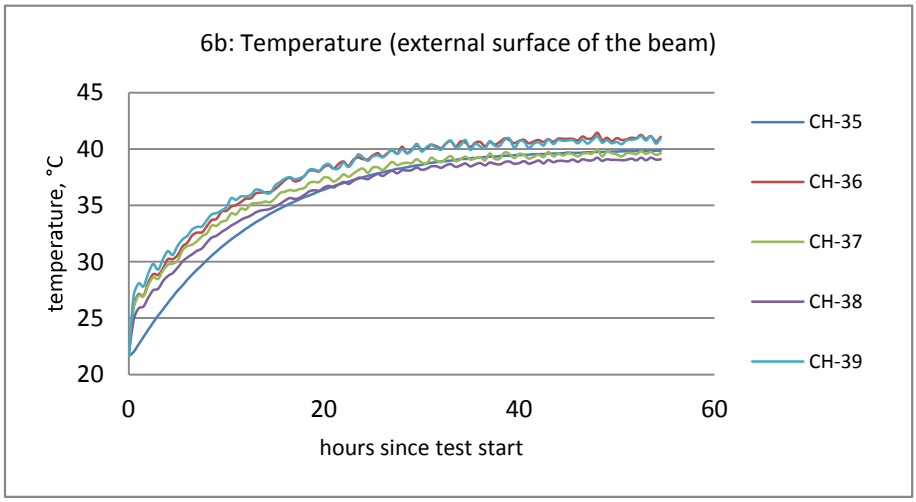
6b: Temperature (external surface of the beam)
temperature, °C
45
40
35
30
25
20
0
20
40
60
hours since test start
CH-35
CH-36
CH-37
CH-38
CH-39

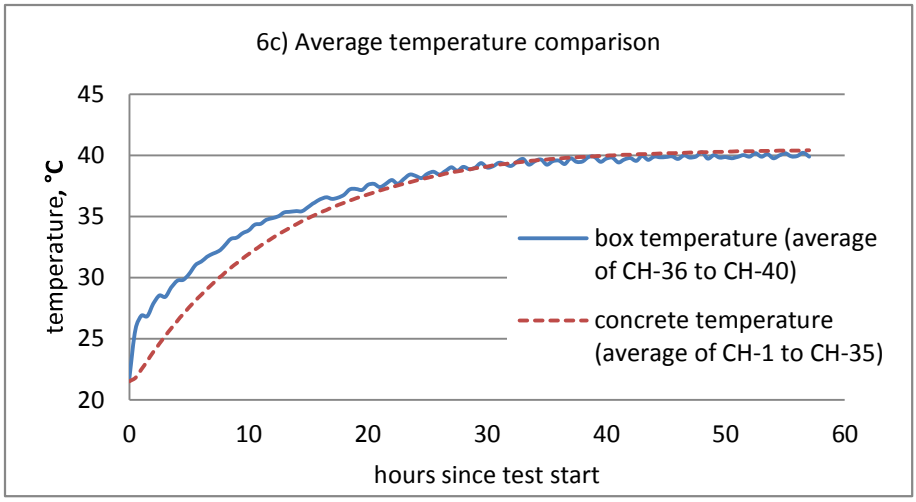

Figure 6 Temperature monitoring (Results from thermocouples)

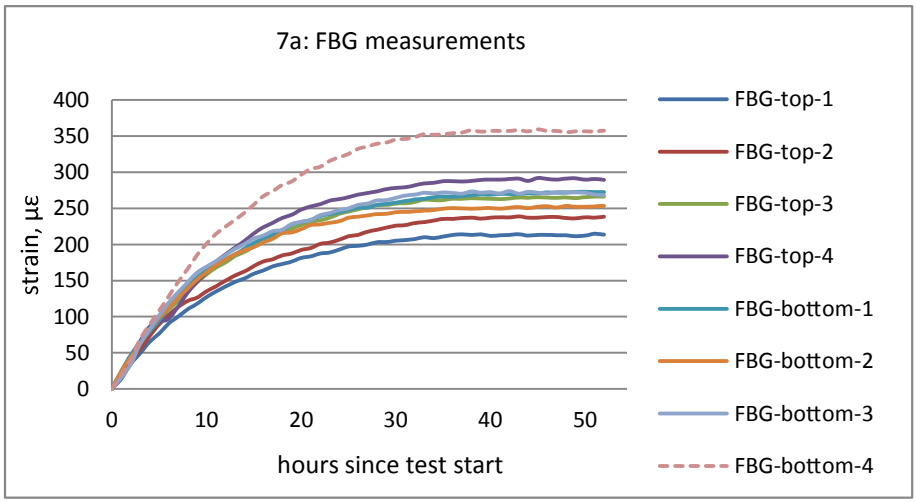

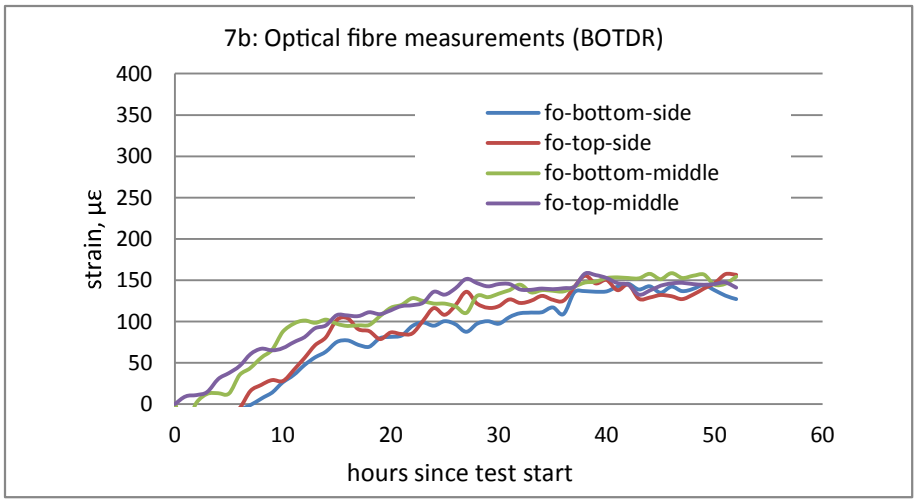

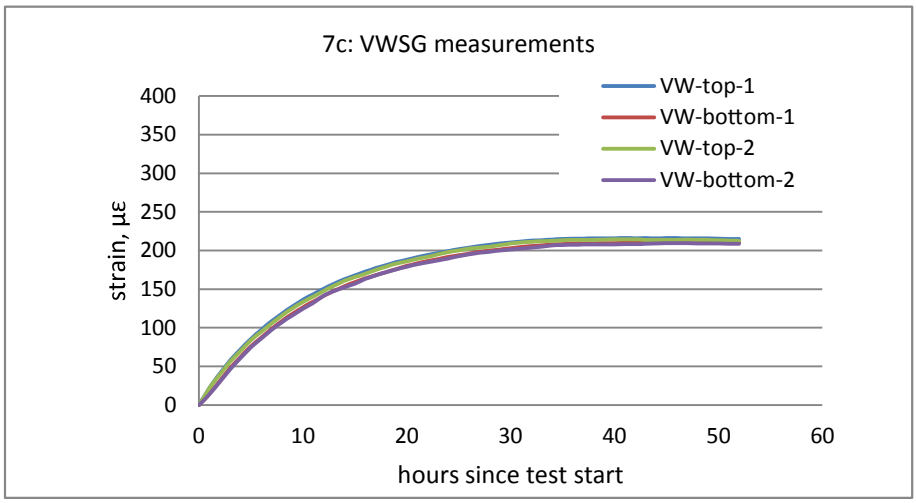
7c: VWSG measurements
VW-top-1
VW-bottom-1
VW-top-2
VW-bottom-2
strain, με
400
350
300
250
200
150
100
50
0
0
10
20
30
40
50
60
hours since test start

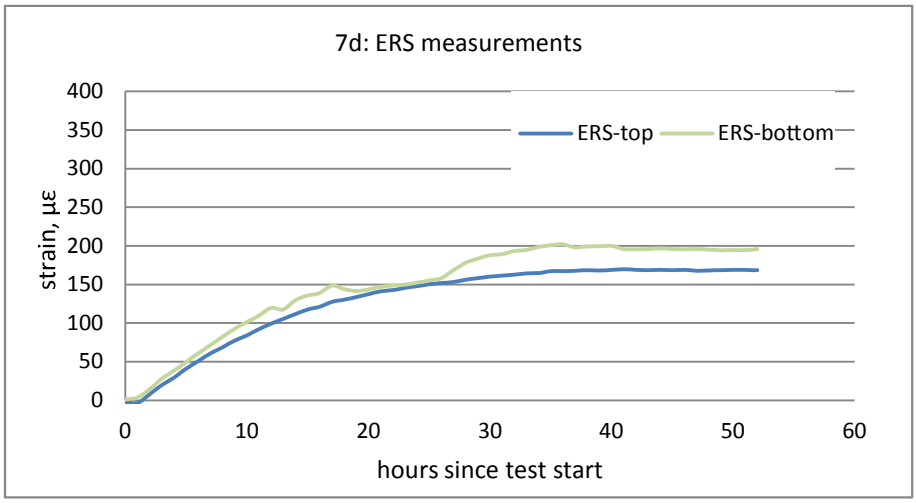
7d: ERS measurements
ERS-top
ERS-bottom
strain, με
400
350
300
250
200
150
100
50
0
0
10
20
30
40
50
60
hours since test start

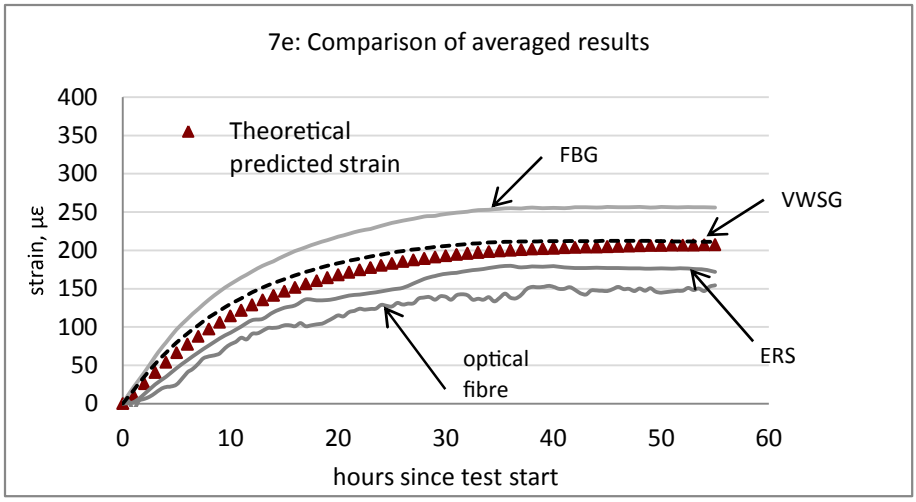

Figure 7 Temperature compensated strain results

Figure 7a to 7d show the results from each of the strain measurements after compensating for temperature effects from the different sensors. Temperature effects were considered by adopting a temperature calibration factor. This factor was different from one type of sensor to another and in this experiment was mainly obtained from manufacturers. It is clear from the plots that there is relatively little difference (maximum of 15%) (apart from the FBG sensors which will be discussed in later sections) between the measurements of the different sensors of the same type, therefore the measurements of each sensor type can be represented by an average line for better comparison. Figure 7e plots the average values from the different sensor types together with the theoretical predictions of strain obtained (using a thermal expansion coefficient of concrete of 11με/°C (Neville, 1997)). The average FBG and VWSG measurements produced a smooth curve when plotted against time whereas the other sensors showed more fluctuations in the results. FO sensors, which had a longer measurement time (around 20 minutes per measurement compared to instantaneous measurements for the other sensors), show larger fluctuations suggesting that FO sensors are unlikely to give stable measurements under rapidly changing temperature conditions. The results presented in Figure 7e were filtered measurements, in which a moving average was applied over each 10 data points along the length. The

strain measurements from all the sensors, after allowing for temperature effects, were within ±25 from the calculated concrete thermal strains.

3.2. Temperature gradient experiment

Temperature measurements from the thermocouples inside the beam (Figure 2 taken over a 95-hour period are presented in Figure 8a to 8c. These show that the thermocouple measurements at the same levels (same depths through the beam) are very consistent hence average values can represent the temperature at different levels. The lines labeled as Concrete-top, Concrete-middle and Concrete-bottom in Figure 8d refer to the average measurements from all the thermocouples at the top, middle and bottom parts of the beam respectively. For this part of the experiment, the beam was subjected to two heating processes in two stages. In stage 1, the air temperature inside the box was heated up to a maximum of 46°C in 10 hours with the top surface temperature of the beam reaching a maximum of 42°C (Figure 8d). In stage 2, the air temperature inside the box was kept at 46°C with the external fan (shown in Figure 5a) on the underside switched on (24 hours after the test had been started) to accelerate the airflow at the bottom surface of the beam in order to maximise the temperature difference between the top and bottom surfaces of the beam. The process finally stabilised at approximately 14°C difference between the top and bottom surfaces and about 7°C difference between the top and bottom reinforcement layers inside the concrete beam.

The strain results obtained from sensors are shown in Figure 9 for the top, middle and bottom parts of the beam respectively. Each line shown in Figure 9a and 9b is the average plot for all the sensors of the same type; the strain measurements obtained from the same type sensors at the same depth in the beam were very consistent. The theoretical strain for the concrete was again calculated assuming a thermal expansion coefficient of 11με/°C. Despite the sensitivity of each sensor, the difference in conductivity of concrete and steel created a complicated heat conduction process in the bottom part of

the beam, which caused a bigger variation in the bottom measurements (30

The results from FO, which requires longer sensing time, can clearly demonstrate the unavoidable effect of temperature changes on strain measurements. The measurements from the ERS in particular were 50 lower than measurements from other sensors and the theoretical values. This could be due to ERS creep when subjected to increasing temperature.

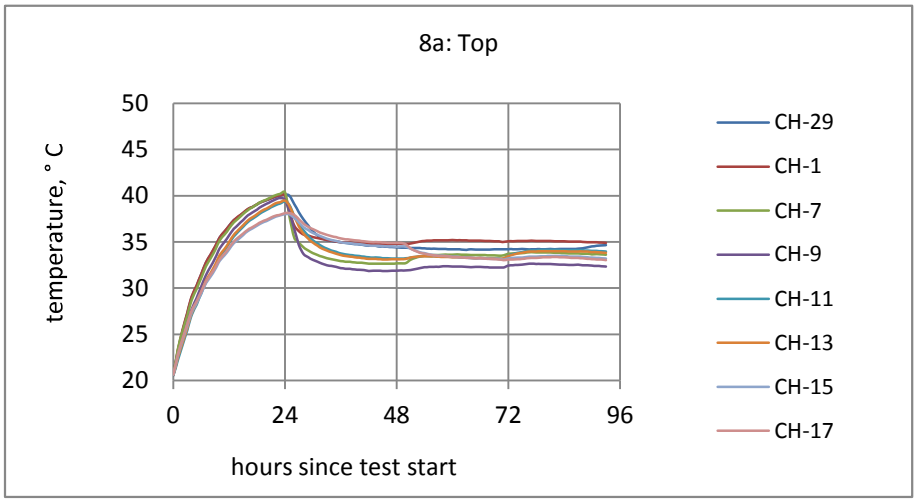

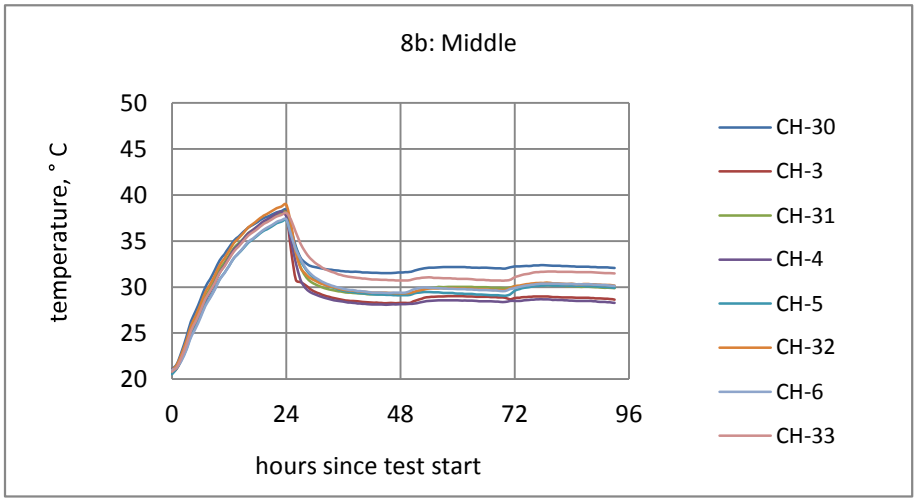

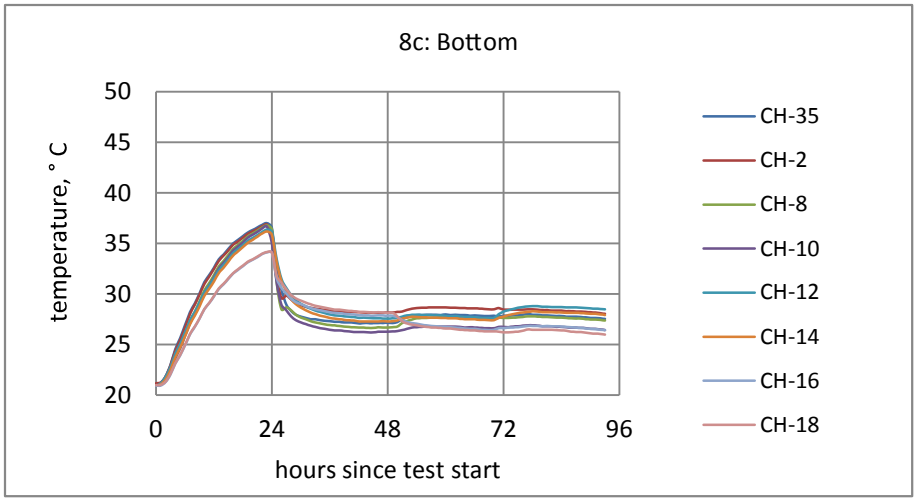

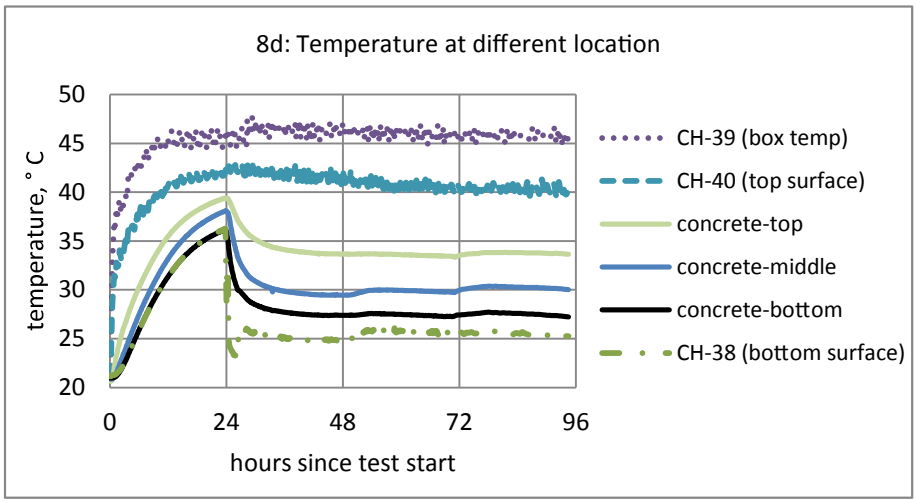

Figure 8 Temperature gradient through beam depth

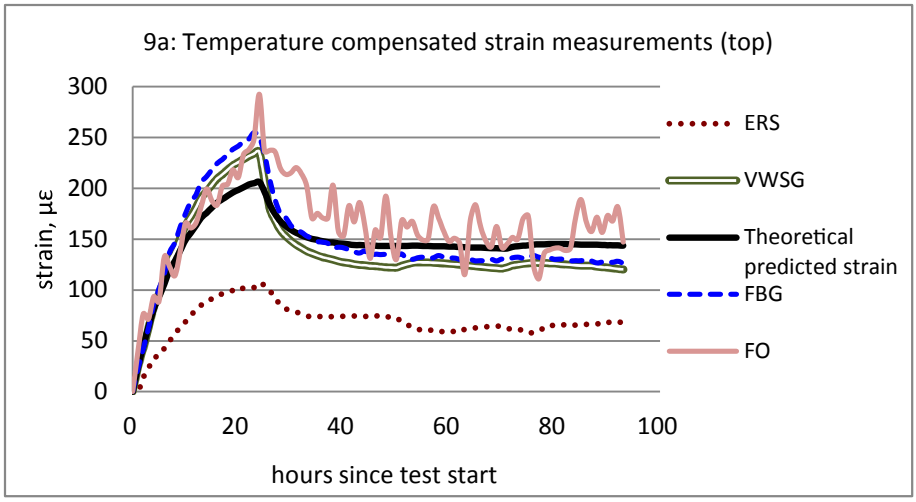

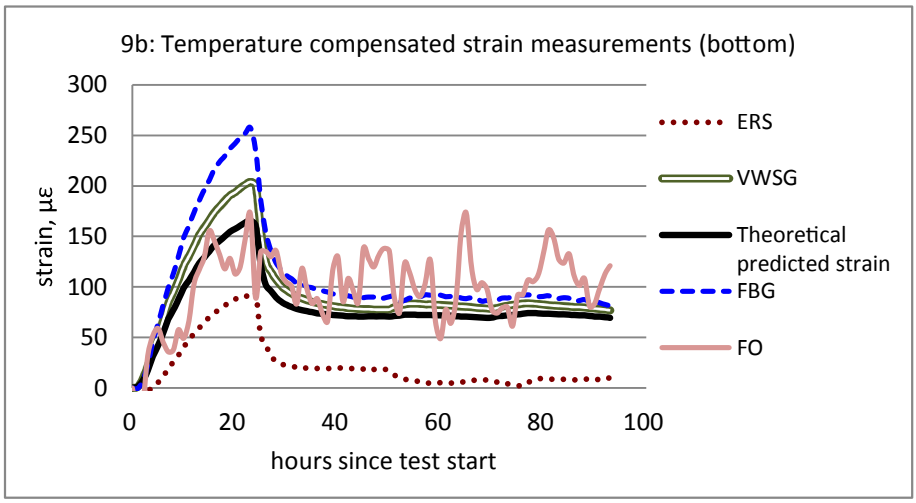

Figure 9 Strain measurements of instruments inside the concrete beam subjected to dynamic temperature environment

4. Discussion

4.1. Fibre Bragg Gratings (FBGs)

FBGs are essentially reflectors built inside the core of an optical fiber. The reflectors are made by permanently altering the refractive index of the core. Each FBG reflects a certain narrow slice of

spectrum. Such slices typically have a smooth Gaussian shape; the centre (i.e., top) of the reflected Gaussian peak is what is used to make measurements. The FBG's peak shifts (to a higher or lower center wavelength) when either the fiber is strained or its temperature changes.

The measurements obtained from the sensor labeled as "FBG-bottom-4" (the bottom sensor on the right as shown in Figure 1d) showed a significant variation (about 100με) from all the others at the maximum temperature to which the concrete beam was subjected (Figure 10a). Looking into the spectrum response of this particular FBG, three peaks were noticed for measurements above 32°C, so the analyser tracked different peaks at different times leading to large measurements. Measurements from the rest of FBG sensors varied by approximately 10

Figure 10b the average is 275με ± 48με). The linear nature of the plots in Figure 10a and 10b may suggest that this variation between the FBG measurements is due to the effect of using inaccurate strain calibration coefficients, however, other factors such as sensor installation effects (bonding between the sensor and the steel reinforcement) and localised effects (effect of the localised concrete strains on the sensor) could have also influenced the measurements. Temperature compensation is conducted by using a temperature calibration factor (also called the thermal-optical constant) which relates the shift in wavelength of the Gaussian's peak to temperature change (Kreuze,2013). For a given temperature change the corresponding wavelength shift is calculated and subtracted from the total shift. In Figure 10b, which shows the temperature compensated FBG strain measurements, inconsistency between the FBG sensors is observed; a number of factors might have caused such variation.

1) The resolution of the recorded temperature measurements (temperature measurement resolution): In this case, approximately ±8με difference could have been caused due to the ±1°C thermocouple resolution.

2) The temperature calibration of the FBG sensors: standard practice is to apply a conversion coefficient to the frequency shift output from the sensors. Manufacturers typically use a single conversion coefficient for all the sensors supplied (0.017nanometer/°C for the FBGs used in this research). However, thermal calibration tests performed by the authors (described in more detail later) found that a difference of up to ± 2 variation in total) could be measured between individual sensors on the same cable when subjected to the same temperature change. According to the FBG manufacturer's datasheet, a strain of magnitude 1με causes a peak wavelength shift of 1.213 picometer, therefore, at 42°C, the total 4 tion equates to about 24με (±12με).

3) The two factors above could account for 28με of a total discrepancy of 48με discrepancy observed in Figure 10b. The other 20με could be attributed to other effects like the bonding between the FBG sensors, the steel reinforcement and the surrounding concrete; normally assumed to be the same for all the sensors, however, in practice it is not possible to verify that this is the case. In addition, the concrete surrounding the sensors is assumed to behave homogenously throughout but in practice the concrete will have minor variations along the beam resulting in small different bond characteristics with the FBG sensor and the steel.

Measurements of FBG sensors from stage 1 of the temperature gradient test (as detailed in Section 3.2) after temperature compensation are shown in Figure 11. The graph shows that the FBG sensors did not pick up the strain difference due to the 3°C temperature gradient, recorded 24 hours after the start of the test, between the top and bottom reinforcement layers (see Figure 8d). Such a temperature gradient corresponds, in theory, to about 30με strain difference; it is interesting to note that the manufacturer of the FBGs claims a 1~2με strain resolution.

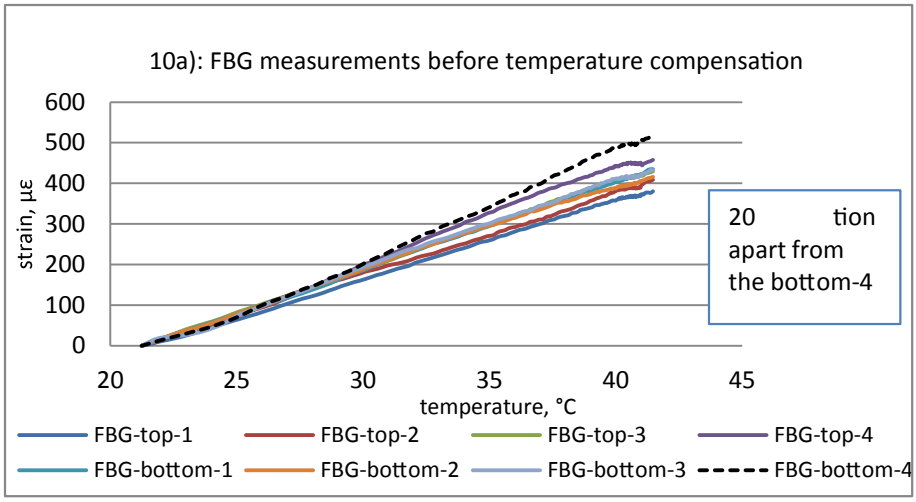

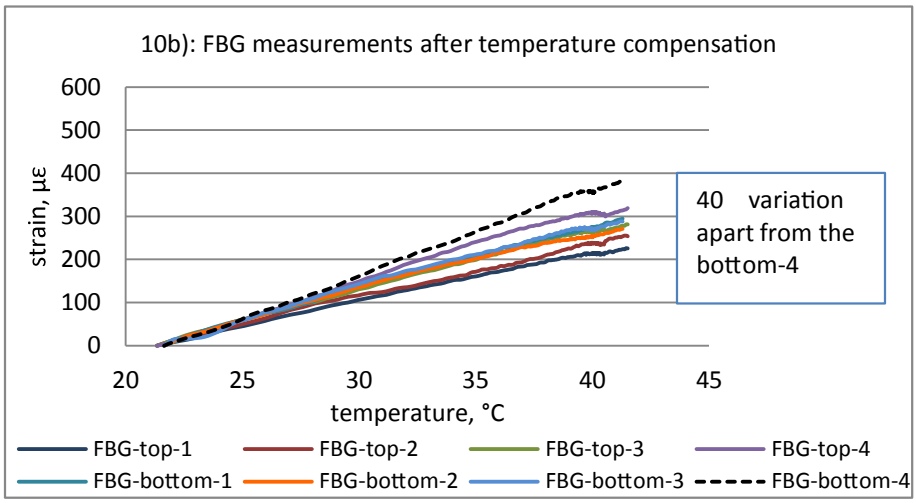

Figure 10 Results of FBG sensors from the constant temperature test

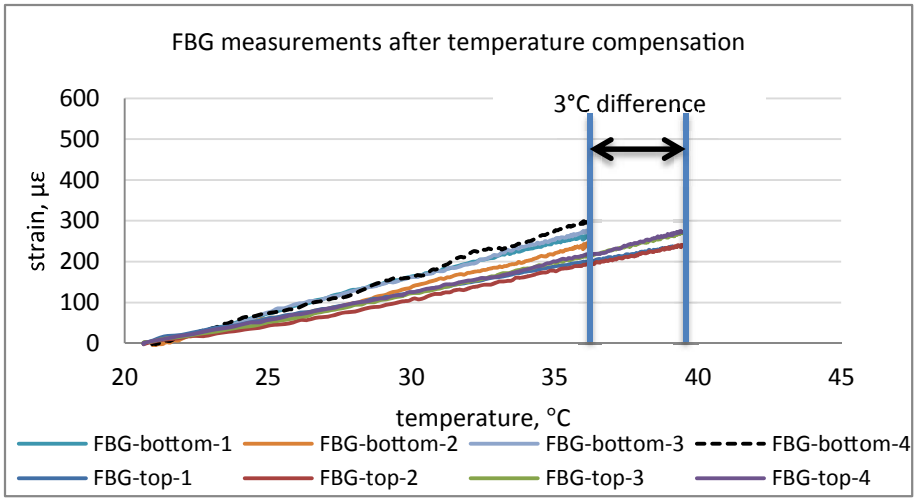

Figure 11 FBG strain measurements from the temperature gradient test (stage 1) after temperature compensation

To better understand the consistency of FBG sensors strain measurements, a temperature calibration test was also carried out by placing a test cable (five FBG sensors manufactured on a single cable) into a water tank as shown in Figure 12. The water temperature was controlled by a heater and measured by three different thermocouples at different locations as shown in the figure. Data from the fourth sensor (FBG-4) were excluded because as temperature increased, it experienced data loss. This might be because the sensor was located close to the heater and the fan (used to distribute heat around), which caused the sensor experienced unusual strain changes. The results, plotted in Figure 13, show a 4 difference between the sensors when subjected to the same temperature change (at 42°C this equates to approximately 24με). This inconsistency reveals that applying an average temperature coefficient to different FBG sensors is insufficient to obtain reliable measurements.

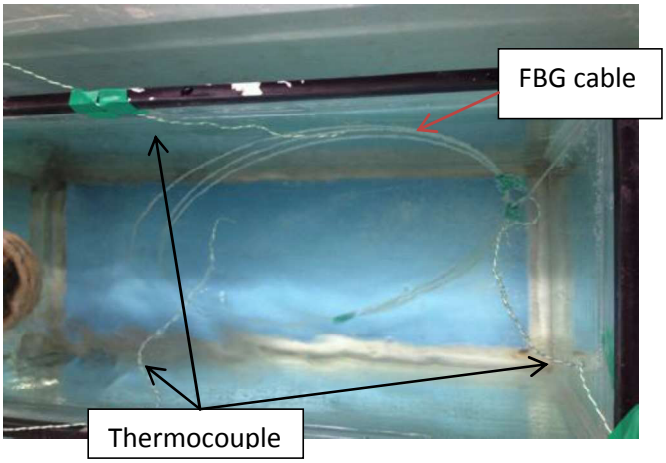

Figure 12 FBG temperature test setup

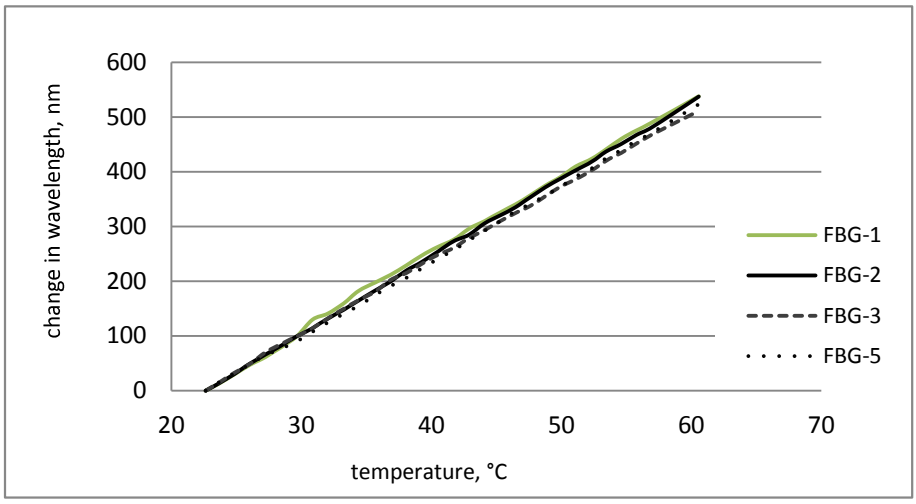

Figure 13 Temperature test results of FBG sensors

4.2. Vibrating wire strain gauges (VWSG)

Compared to the FBG sensors, measurements from the VWSGs exhibited very good consistency throughout all the tests. In particular, for the temperature gradient test, VWSG results clearly indicate the strain difference (that is induced by the temperature difference between top and bottom of the beam as shown in Figure 15, which is not captured by FBG sensors). The raw results from VWSGs had a nonlinear negative relationship between measured strain and temperature as shown in Figure 14. The

thermal output of VWSGs is induced by the difference in expansion of the steel wire in the gauge and the concrete. The thermal output is calculated as follows (with known temperature and thermal expansion coefficient of steel) (Geokon-VWSG Manual):

$$\boldsymbol{\varepsilon = 3.304 \times 10^{-3} B\left(f_1^2 - f_0^2\right) + (T_1 - T_0)C_1} \qquad \textbf{Equation 1}$$

Where B: the batch calibration factor provided by the VWSG manufacturer

f_1, f_0: final and initial frequencies

T_1, T_0: final and initial temperatures

C_1: thermal expansion coefficient of steel (=12.2 με/°C)

Compared to the total raw strain recorded by the VWSG, the steel thermal strain is significantly large and therefore dominates the shape of the graph of temperature compensated measurements as shown in Figure 14b and Figure 15. Even though the linearity in response is achieved by conducting a theoretical calculation, the good agreement between estimated concrete strain and the actual measurements provides strong evidence that the standard temperature compensation method (Equation 1 above) is adequate. A maximum discrepancy of about 10με is noticed in Figure 14b; this is well within the uncertainty due to the temperature resolution measurement of ±1°C. The VWGSs are fixed mechanically to the steel bars, so installation and bonding issues are not expected to have any significant influence.

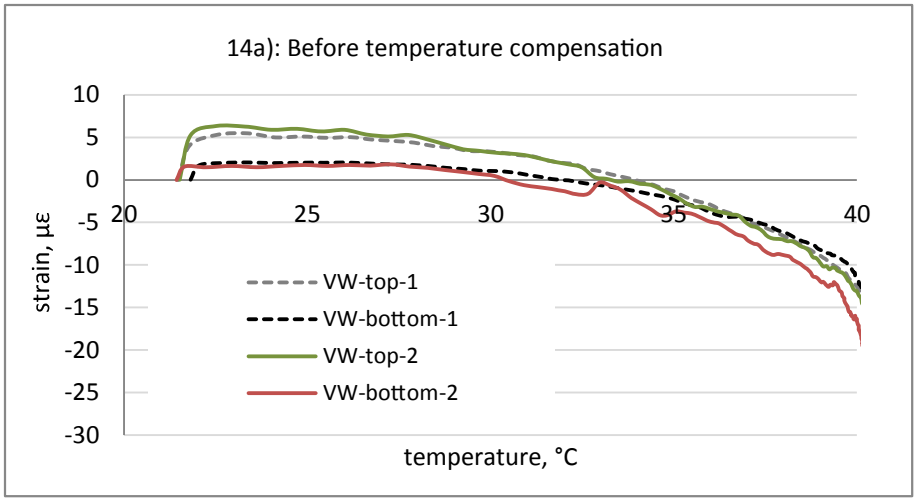

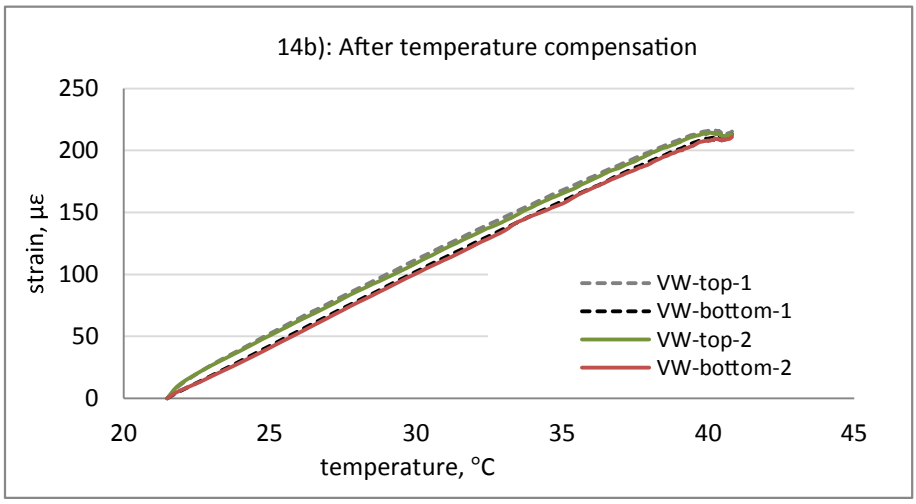

Figure 14 Results of VWSG from the constant temperature test

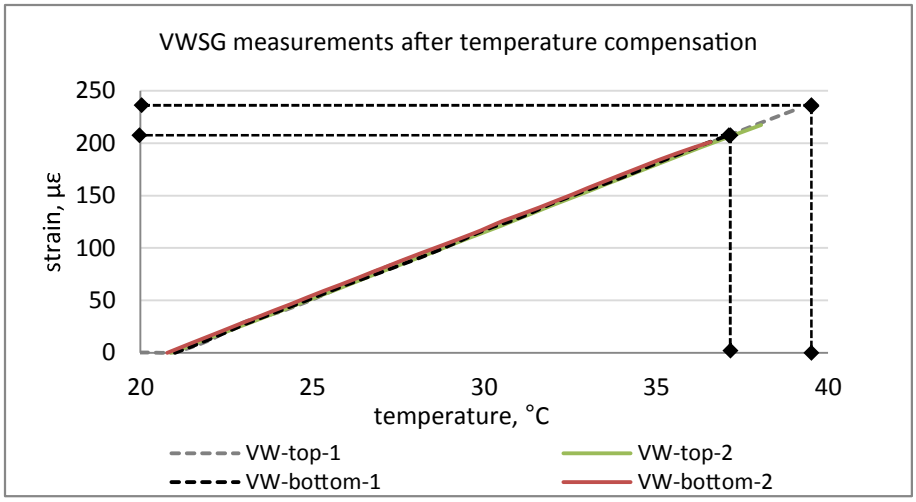

Figure 15 VWSG strain measurements from the temperature gradient test (stage 1) after temperature compensation

4.3. Distributed optical fibre sensing cables

Fibre optic strain sensing technology capitalises the capability of light wave to travel along the entire length of a cable and the strain dependency frequency shift of the backscattered light to provide a continuous and distributed strain sensing solution (Mohamad, 2008). Through the principle of Brillouin Optical Time Domain Reflectometry (BOTDR), when light passes through the fibre optic cables, a small amount of signal will be reflected back to the source as backscattered light. These may come in the form of Rayleigh, Brillouin and Raman backscattering. Within Brillouin backscattering, the peak Brillouin frequency experiences a shift when strain is induced. A linear correlation exists between the frequency shift and strain of the fibre optic cable. With the known time it takes for the backscattered signal to return to source, distance can be measured to a particular point of which the frequency shift or strain was measured. This effectively transforms the fibre optic cable to be the sensor itself, thus providing a continuous strain profile along its entire length. As shown in Figure 1, the beam was instrumented using fibre optic cables at varies locations along the beam. For strain measurement, the Fujikura Reinforced

Ribbon Cable (JBT-03813) was used; the nylon coating and the inner glass cores are fixed together (known as tight-buffered) to ensure that the strain applied on the outer nylon sheath is transmitted into the cores. For temperature measurement, the standard loose-tube Unitube cable was used; the optical cores in this cable are surrounded by a gel and so the strain applied on the outer sheath does not get transmitted into the cores. Figure 16 shows the cross-sections of the two cables.

Comparison of temperature profiles obtained by the distributed Unitube fibre optic temperature cable with the discrete temperature measurements obtained by the thermocouples (locations of thermocouples shown in Figure 17) is shown in Figure 18 at different times during the test. The BOTDR measured strain from the Unitube cables are converted into temperature by using the conversion factor 23.67με/°C (Mohamad et al (2014). From the constant temperature test where heat is gently conducted through the beam, as expected, temperature increased very quickly at beginning, corresponding to bigger jumps from one profile to another. Comparing FO measured temperature with the thermocouple readings, an average 2°C difference was observed (Figure 18a). This is perhaps not surprising given that the resolution of the fibre optic measurement device using the Unitube cable is about ±100με which translates to about 4°C uncertainty in temperature measurement. This is in addition to the ±1°C uncertainty associated with the temperature measurement. Mohamad et al. (2014) embedded a fibre optic Unitube cable and thermocouples inside a concrete beam to measure the temperature change (using the two different sensors simultaneously) during the curing process following casting of the beam. When compared, the fibre optic cable measurements and the thermocouples' measurements had a difference of about 1.5°C; this is similar to what was observed in the tests reported in this paper.

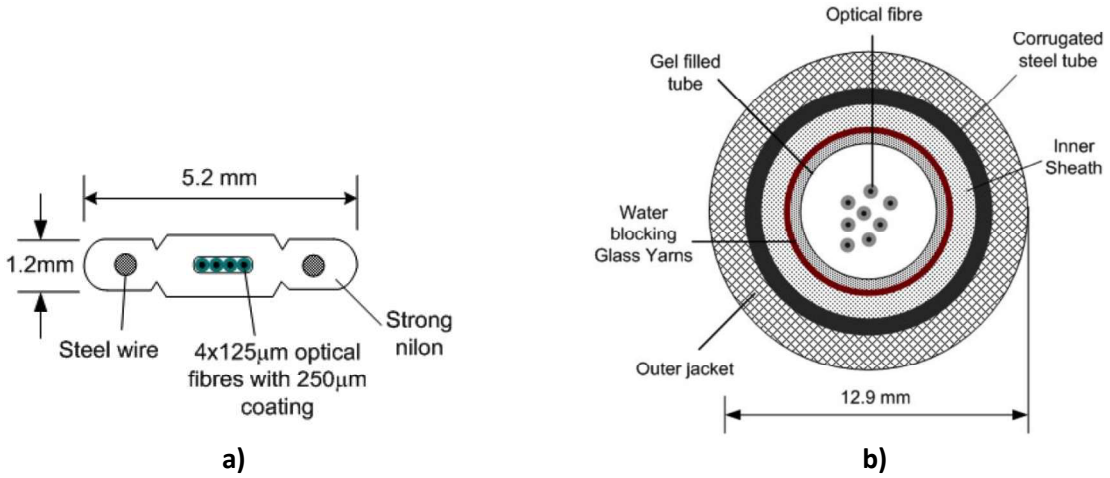

Figure 16 (a) The Fujikura Reinforced Ribbon cable and (b) The Unitube cable

For the temperature gradient test where heat is conducted from the top to the bottom of the beam, Figure 18b shows the results at the start of the temperature gradient test as well as at 4, 10 and 24 hours after the test start (24hours corresponds to the end of Stage 1). The FO temperature measurements, under such a relatively dynamic temperature environment, had about 5°C difference when compared to the thermocouples. Distributed FO temperature measurements are not sufficient to provide accurate local temperature information. However with the ability to provide a continuous temperature profile along the cable length, FO temperature cables are very useful in assisting engineers to assess the general temperature condition of structures. Figure 18b shows that the sensors in the middle of the beam measured slightly lower temperatures in comparisons the outer ones. The underside of the beam had better air flow in the middle compared to the ends due to the experimental setup required to hold the beam and insulation around it. This could explain why the middle was slightly lower in temperature compared to the sides.

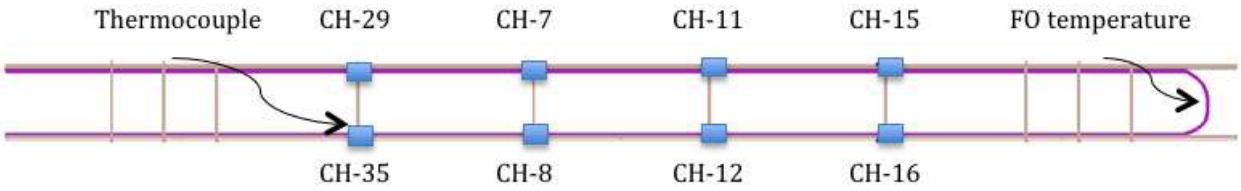

Figure 17 Locations of thermocouples for temperature measurements comparison

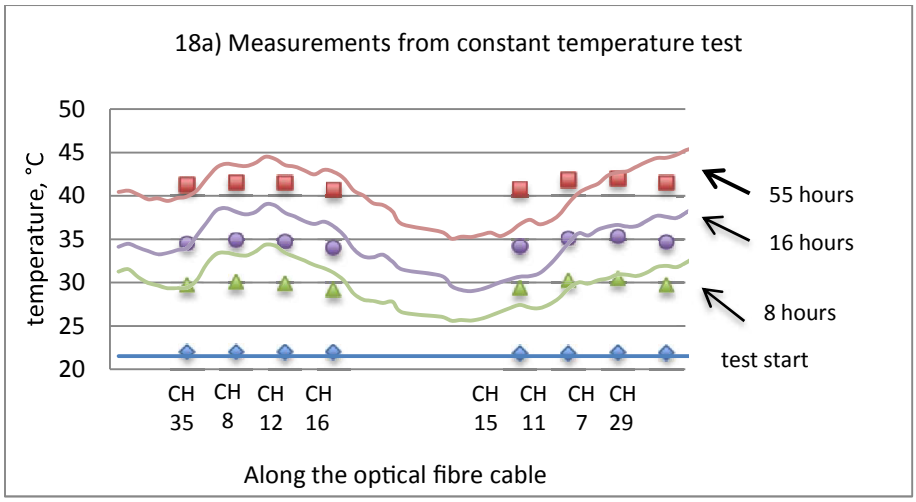

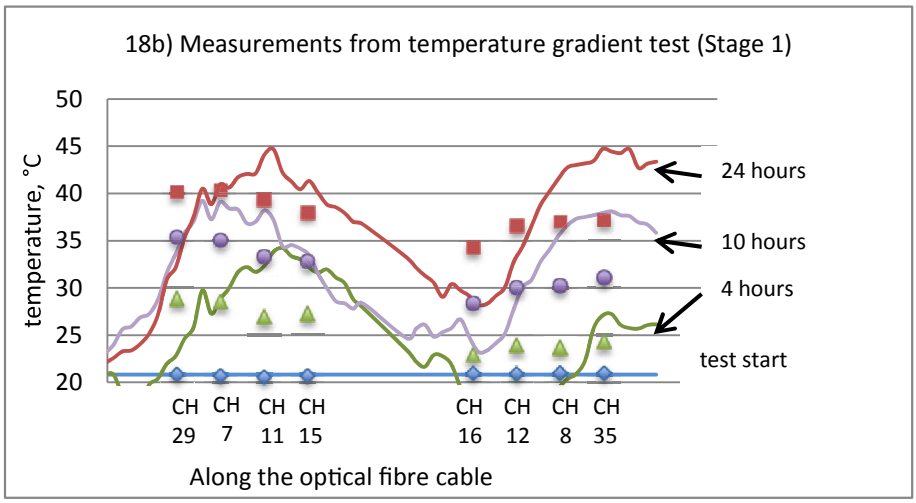

Figure 18 Comparison of temperature measurements from FO temperature cable and thermocouples

There are a number of methods used to conduct temperature compensation depending on the specifics relating to the type of optical cable, optical fibre analyser and method of installation (Mohamad, 2012). A loose-tube standard telecommunications cable (Unitube) was installed next to the Fujikura strain sensing cable (JBT-03813) in order to conduct temperature compensation.

Mohamad (2012) showed that the thermal strain ($d\varepsilon_{thermal}$) can be derived from the following equation:

$$d\varepsilon_{thermal} = (\alpha_a + \alpha_{jacket})\, dT \qquad \text{Equation 2}$$

where $\alpha_a = 19.47 \times 10^{6}$m/m°C (BOTDR intrinsic thermal coefficient in a bare single-mode silica fibre) and α_{jacket} is the thermal expansion coefficient of the fibre induced by the thermal stresses within the jacketed optical fibres. When the optical fibre cable is fully embedded in concrete, the jacket thermal expansion becomes less important as the concrete dominates and hence α_{jacket} can be replaced by $\alpha_{concrete}$ the thermal expansion coefficient of concrete (Mohamad et al, 2014). The thermal strain can then be subtracted from the total strain measured by the BOTDR analyser. For temperature compensation of distributed strain fibre optical measurements, two commonly used data processing methods are compared in this paper:

1) Subtracting the thermal strain from the total strain on a point by point ('pt to pt') basis along the sensing length.
2) Averaging the thermal strain over a 1m length and then subtracting this value from the total BOTDR measured strain over the same 1m length ('average 1m').

Figure 19 demonstrates the comparison of results from both experiments after compensating for temperature effect with different methods. The 'middle' presents results obtained from the middle strain cable which is barely embedded in concrete and 'side' means data from side cable that is attached to reinforced steel bar as shown in Figure 1d. In the constant temperature experiment, for temperatures

beyond 33°C, strain measurements from both cables with either temperature compensation method are giving close results with an average variation of less than 25με. However, for temperatures between 20°C to 30°C, the result from side cable with “average 1m” temperature compensation methods shows a particularly lower strain measurement. Correlated back to the temperature profile in Figure 6, the specimen and fibre cable at this period of time were subjected to a rapidly temperature change condition. Considering the operational characteristics of the BOTDR Analyer with the spatial resolution of 0.5m and sensing time of ~30 seconds, the large variation in this part of the graph is within the acceptable limits of the BOTDR.

Under a rapid temperature-changing environment, a larger variation in temperature results in a higher uncertainty in thermal strain measurements and thus a different observation is made from the temperature gradient test. As shown in Figure 19b, the linearity of the measured strain to temperature graph is reduced, which implies that the material that the cable was attached to is the main factor influencing the final results in this case. This is further confirmed by measurements from bottom part of the beam: a better coherence is observed between results obtained from the two temperature compensation methods at this level while a clear difference appears between results from the middle cable and side cable.

Therefore, under a constant temperature condition where the concrete is gradually heated up, whether to install the FO cable to reinforcement or barely in concrete will give insignificant difference in final measurements. Alternatively, for situations where heat is quickly conducted through the concrete, the material that the FO cable is attached to has a significant contribution to the final measurements. The temperature compensation methods are found to have minor effect on either cable in either situation.

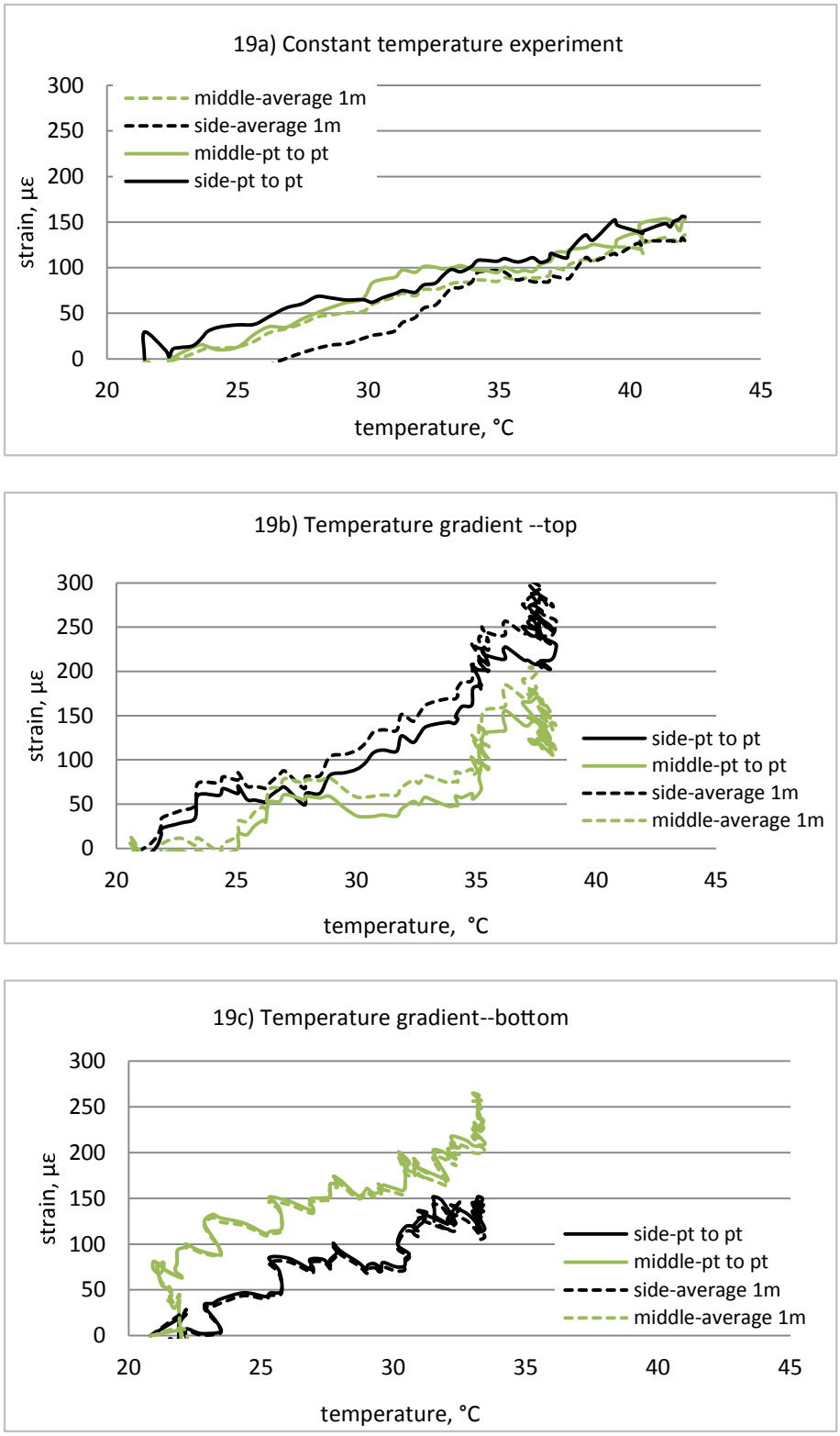

Figure 19 FO strain measurements after filtered (temperature compensated)

5. Conclusions

Civil engineering infrastructures, including bridges, buildings, pipelines, etc., begin to deteriorate once they are built and operated. They could also be subjected to unexpected loading scenarios and/or frequent changes in the environmental conditions. The importance of monitoring the health of these civil infrastructures over time cannot be overstated; maintaining safe and fully functional civil infrastructures for daily use is vital for the well being of all societies. A wide range of commercially available strain sensors are frequently used to record the performance of civil engineering structures with time and/or loading; however, a common problem faced when using these sensors is to distinguish strain changes experienced by the structure due to a temperature change from strain changes that occur due to other causes.

In this research, four types of strain sensors including (i) electrical resistance strain gauges (ERSs), (ii) vibrating wire strain gauges (VWSGs), (iii) Fibre Bragg Gratings (FBGs), and (iv) distributed fibre optic strain sensors (FO) were embedded inside a reinforced concrete beam to test their performance under thermal loading. The thermal loading included a constant temperature test where the whole beam was subjected to temperature change and a temperature gradient test where only the top surface of the beam was subjected to increasing temperature while the bottom surface was exposed to room temperature.

Comparison of the results that included compensation for temperature effects by following the guidance from sensor manufacturers demonstrated an average of 25 tion in measurements between the different types of sensors under the constant temperature test. For the temperature gradient test, an even larger variation (30 in measurements was observed.

Correctly understanding the characteristics of the different sensors would significantly increase the confidence in the measurements obtained; based on results obtained from the test reported in this paper, the VWSGs produced the most stable and reliable results (compared to the theoretical calculations) among the four sensors. It was demonstrated that the measurements from the FBG sensors could show a significant amount of variation, which could be reduced substantially by calibrating each individual sensor separately before installation and following strict installation procedures. The paper demonstrated that ERSs could be highly unreliable due to their high sensitivity to the test environment (ie, the installation surface and the covering material); this raises questions about their long term monitoring viability inside concrete structures.

The FO sensors, with the advantage of providing continuous temperature or strain profiles, were unable to give highly accurate temperature measurements inside concrete. In particular, a 5°C difference was observed under a dynamic temperature environment. Thermocouples, in contrast, were highly reliable in comparison; however a large number of thermocouples would be required to monitor large concrete structures in practice with a much higher demand for labour during installation and cable routing. However, for more stable thermal conditions where the temperature does not change quickly over short periods of time, the continuity of the FO sensing provides a major advantage. The inability of FO sensors to detect localised deformation due to the spatial resolution limitation can be overcome by using properly calibrated VWSGs or FBG sensors where required.

Acknowledgement

The authors would like to acknowledge Dr. Peter Long, Martin Touhey and the Engineering Structures Laboratory technical staff at University of Cambridge for their assistance through the experimental program. The authors are also grateful to the Cambridge Center for Smart Infrastructure and Construction for supporting this research project.

References

Bao, X. and Chen, L. (2011). Recent Progress in Brillouin Scattering Based Fiber Sensors, Sensors 2011, 11(4), 4152–4187.

Chen, B., Maher, M.H., and Nawy, E.G. (1994). Fiber-optic Bragg Grating Sensor for Nondestructive Evaluation of Composite Beams, ASCE Journal of Structural Engineering, 120 (12), 3456–3470.

Geokon Incorporation (2013). Instruction Manual, Model 4200 Series, Vibrating Wire Strain Gauges, http://www.geokon.com (accessed on 23rd/05/2013).

Hoult, N.A., Bennett, P.J., Middleton, C.R. and Soga, K. (2009). Distributed Fibre Optic Strain Measurements for Pervasive Monitoring of Civil Infrastructure, Proceedings of the 4th International Conference on Structural Health Monitoring of Intelligent Infrastructure (SHMII-4), edited by Urs Meier, Bernadette Havranek and Masoud Motavalli, 22nd-24th July 2009, Zurich, Switzerland; ISBN: 978-3-905594-52-2.

Kreuze, M. (2013). Strain Measurement with Fiber Bragg Grating Sensors, Report Number S2338-1.en, HBM Gmbh, PO Box 100151, D-64201, Darmstadt, Gemany.

Mohamad, H. (2012). Temperature and Strain Sensing Techniques Using Brillouin Optical Time Domain Reflectometry, Proceedings of SPIE, Smart Sensor Phenomena, Technology, Networks, and Systems Integration 2012, edited by T. E. Matikas, K. J. Peters, and W. Ecke., San Diego, California, 11th March 2012, vol. 8346,1-13.

Mohamad, H. (2008). Distributed Optical Fibre Strain Sensing of Geotechnical Structures, Ph.D. Thesis, Cambridge University Engineering Department, United Kingdom.

Mohamad, H., Soga, K. and Amataya, B. (2014). Thermal strain sensing of concrete piles using Brilloiun optical time domain reflectometry, ASTM Geotechnical Testing Journal, vol 37, Issue 2 March 2014, 333-346.

Neild, S.A., Williams, M.S. and McFadden, P.D. (2005). Development of a Vibrating Wire Strain Gauge for Measuring Small Strains in Concrete Beams, Strain 2005, volume 41 (1), 3–9.

Neville, A. M. (1997). Properties of Concrete, Prentice Hall (publishers), 378-384, ISBN 9780470235270.

Othonos, A. and Kalli, K. (1999). Fiber Bragg Gratings: Fundamentals and Applications in Telecommunications and Sensing. Artech House (publishers), 98-99, ISBN 9780890063446.

Schwamb T. (2010). Optical Strain Sensing for Piled Foundations at Ninewell's Bridge, M.Phil. thesis, Cambridge University Engineering Department, United Kingdom.

Sreeshyiarn, P., Ravisankar, K., Parivallal, S., Kesavan, K. and Sridhar, S. (2008). Condition Monitoring of Prestressed Concrete Structures Using Vibrating Wire Sensors, International Journal of COMADEM, 11(3), July 2008, 46-54.

Webb, G.T. (2010) Structural Health Monitoring of Bridges, Fourth-year Masters project report, Cambridge University Engineering Department, United Kingdom.

Webb, G.T. (2011). Structural Health Monitoring, First Year PH.D. Report, Cambridge University Engineering Department, United Kingdpm.4